Measurement of the electron-spin susceptibility of Li, Cu, and Ag via transmission conduction-electron-spin resonance in metallic bilayers

D. C. Vier, D. W. Tolleth,* and S. Schultz
Department of Physics, University of California, San Diego, La Jolla, California 92093
(Received 13 May 1983)

A new technique is discussed which utilizes conduction-electron-spin resonance (CESR) in metal bilayers to determine the electron-spin susceptibility of metals. Transmission electron-spin resonance measurements are performed on bilayers made from various pairs of the metals lithium, sodium, potassium, copper, and silver. These measurements allow a determination of the ratio of the electron-spin susceptibilities of the two metals constituting the bilayer. Combining previously measured values of the electron-spin susceptibility of Na and K with our bilayer data, and performing a least-squares analysis, yields values of the electron-spin susceptibility of Li, Cu, and Ag. The resulting values are $(2.29\pm0.13)\times10^{-6}$ cgs volume units for lithium, $(1.35\pm0.06)\times10^{-6}$ cgs volume units for copper, and $(0.86\pm0.04)\times10^{-6}$ cgs volume units for silver. These values agree with theoretical estimates and other experimental determinations. The self-consistency of our results also supports the reliability of our technique. This technique is potentially applicable to all metals for which CESR can be observed, and we discuss some possible candidates for future bilayer CESR susceptibility measurements.

I. INTRODUCTION

A subject of considerable theoretical interest in solid-state physics is the manifestation of electron-electron interactions in the physical characteristics of metals. One property of metals for which the effects of many-body interactions are amenable to calculation is the electron-spin susceptibility χ, which differs from the value deduced from free-electron theory, χ_0.[1] According to the Landau theory of Fermi liquids, for an interacting electron gas, subject to the assumption of spherical symmetry, this difference is generally expressed as an enhancement given by

$$\chi/\chi_0=(g_s/g_0)^2(m^*/m)(1+B_0)^{-1}\ ,$$

where g_s is the electron-spin g factor of the interacting gas, $g_0=2.0023$, B_0 is the first Landau spin-interaction coefficient, and m^*/m is the ratio of the electron effective mass to the free-electron mass. Both B_0 and m^*/m include electron-phonon contributions and m^*/m must also include the band mass. Calculations of the enhanced susceptibility χ can be tested by comparison with measurements of the electron-spin susceptibilities of metals, thereby testing theoretical models of many-body effects.

The most straightforward method for measuring the enhanced susceptibility χ would be to measure the dc susceptibility directly. This is difficult since the spin susceptibilities in metals are weak and there are competing contributions to the total susceptibility which are generally larger than the contribution due to the electron spin. These include the Landau diamagnetism of the electrons and the susceptibility of the ion cores.

Another measure of χ involves a determination of the area under the conduction-electron-spin resonance (CESR) curve. This method is difficult as it requires both measurement of the absolute CESR amplitude and integration of the CESR line shape over many linewidths to achieve accurate results. Despite these difficulties this procedure has been used for Li and Na,[2] but is not readily extendable to other metals.

Spin-wave and de Haas–van Alphen (dHvA) measurements have also been interpreted to deduce the spin susceptibility of metals, but each method has drawbacks and experimental limitations. The interpretation of the measurements is dependent on the accuracy of various many-body theories describing metals. For spin-wave measurements these include the Platzman-Wolff and Wilson-Fredkin theories,[3] while dHvA measurements rely on the standard one-electron theory due to Lifshitz and Kosevitch.[4]

Resolved spin-wave measurements of χ have only been possible in Na,[5] K,[5] and Rb (Ref. 6) by transmission-electron-spin resonance (TESR). The reason for this is that these measurements require $\omega\tau\,|B_0/(1+B_0)|\gg1$, where ω is the applied frequency and τ is the momentum relaxation time. For many metals, such as Cu and Ag, $|B_0|\ll1$ and thus the above condition is not readily satisfied at typical CESR frequencies. For lithium, although B_0 is appreciable (-0.230), the $\omega\tau$ of existing material is less than 1 at ~9 GHz and thus resolved spin waves are not observed. However, there is a related method which uses TESR data in the regime of completely damped spin waves $[\omega\tau\,|B_0/(1+B_0)|\ll1]$ to determine χ/χ_0.[7,8] This method has been applied to lithium and sodium, but has large experimental uncertainties. The χ/χ_0 of lithium has also been obtained by interpretation of TESR data in the regime of partially resolved spin waves $[\omega\tau\,|B_0/(1+B_0)|\simeq1]$.[7]

de Haas–van Alphen measurements of χ have been undertaken for the alkali and noble metals,[9–12] with the exception of lithium.[13] However, dHvA measurements only determine a series of possible values for χ/χ_0, and thus

other experiments or reliable theoretical predictions of χ/χ_0 are necessary to choose the correct value. Another limitation of the dHvA data is that each measurement is for a single extremal orbit on the Fermi surface. Na and K have isotropic Fermi surfaces to within 1—2% and thus for these metals dHvA data provide reliable measurements in this respect. However, Cu and Ag have Fermi surfaces which are quite anisotropic. Thus the dHvA data for these metals must be appropriately averaged over crystal orientations to yield the spin susceptibility.

Another technique for the measurement of χ involves TESR measurements on dilute local-moment alloys. By observing the coupled conduction-electron—local-moment resonance properties as a function of local-moment concentration and temperature, a value of χ can be obtained for the conduction electrons of the host metal, once the local-moment susceptibility is known. This procedure has thus far been utilized for the local-moment alloys CuCr, CuMn, and AgMn.[14–16] However, the method of analysis is sufficiently complex that the deduced χ's cannot be regarded as reliable compared to the new method reported here.

In this paper we discuss an application of TESR that allows the measurement of a ratio of susceptibilities of two metals which comprise a bilayer sample. The method is applicable to all metals in which CESR is observed. In the TESR technique, microwave power is incident upon one side of a metal sample whose thickness is much larger than the microwave skin depth, and thus the power transmitted through the sample is negligible for applied dc magnetic fields far from the CESR resonant field. However, for magnetic fields near the resonant field, the diffusing electrons can carry a significant amount of power from the incident to the far sample surface. This transmitted power constitutes the TESR signal. For a bilayer made up of two metals having different CESR g values, a single motionally narrowed TESR signal can be observed under appropriate conditions (see Fig. 1).

In Sec. II we show that, if CESR is observed for a metal bilayer under complete motional-narrowing conditions, the observed g value of the motionally narrowed resonance, $\bar{g}$, has a very simple dependence on the spin susceptibilities of the two constituent metals,

$$\bar{g}=\frac{\chi_A L_A/g_A+\chi_B L_B/g_B}{\chi_A L_A/g_A^2+\chi_B L_B/g_B^2}\ . \tag{1}$$

Here subscripts A and B refer to the two constituent metals, g is the conduction-electron g value of the metal, and L is the metal thickness. If one of the constituent metals has a known spin susceptibility, e.g., χ_A, the susceptibility of the other, χ_B, is determined by the measurement of $\bar{g}$.

The significant advantages of this method are as follows. (1) It expands the number of metals for which χ can potentially be measured to include all metals in which CESR can be observed. (2) It simplifies the measurement of χ. With a suitable choice for the reference metal constituent, the task of measuring the weak unknown spin susceptibility of a metal ($\sim 10^{-6}$ cgs volume units) depends only upon accurate determinations of $\bar{g}$ and the thicknesses of both metals constituting the bilayer. (3)

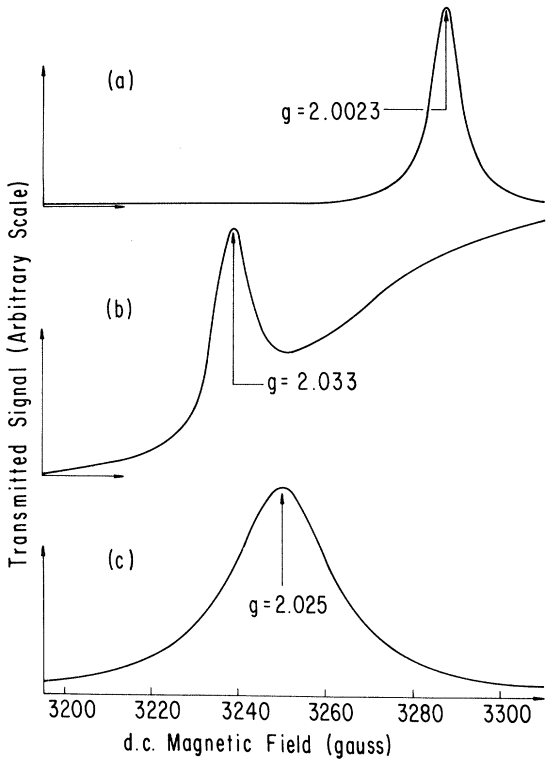

FIG. 1. (a) TESR signal in pure lithium (metal A). (b) TESR signal in pure copper (metal B). (c) TESR signal of a lithium-copper bilayer sample illustrating that the g value of the bilayer TESR line is a χ,L weighting of the g values of the constituent metals as given by Eq. (1).

One may utilize the TESR technique, benefiting from its corresponding advantages for making CESR measurements.[17]

Experimental data are presented for metal bilayers made from various pairs of the metals lithium, sodium, potassium, copper, and silver. Combining our bilayer data with previous determinations of the spin susceptibilities of sodium[5,10] and potassium,[5,9] values of χ are obtained for copper, silver, and lithium. These results are used to deduce values of χ/χ_0 which are then compared with values of χ/χ_0 determined by other experimental methods and by theoretical calculations.

As mentioned, this new method is potentially applicable to all metals for which CESR can be observed. The possibilities for further experiments to determine the electron-spin susceptibility of these metals is discussed in Sec. V.

II. THEORY

A. Bilayer resonant frequency

The resonant g value for CESR in a bilayer under motional-narrowing conditions depends on very few properties of the constituent metals. One of those properties is the electron-spin susceptibility χ of each metal. However, for the bilayer TESR method to be used to obtain an accurate susceptibility determination, the resonant g values of

each metal must be sufficiently different. That is, the accuracy with which χ can be determined is governed by the ratio of the separation of the individual resonances to the width of the resulting bilayer resonance. We now give a physical argument for Eq. (1) (Ref. 18) which is correct under conditions of complete motional narrowing and negligible spin relaxation at the boundaries. We will then discuss the experimental conditions under which complete motional narrowing can be achieved for bilayer metallic samples. For data analysis, the computer simulation described in Sec. II B was used in all cases to eliminate possible error due to incomplete motional narrowing. [For our samples, Eq. (1) agreed with these computer simulations to within $\sim 5\%$.]

Consider the effect of adding an additional electron to a metal bilayer. It resides at the common Fermi level of the two metals, and thus by randomly diffusing throughout the bilayer, the average amount of time it spends in one of the metals is proportional to the *number* of states at the Fermi level $N(\epsilon_F)$ of that metal (for infinite time averages). The same is true for all electrons in the bilayer at (or near) the Fermi level, and it is these electrons that contribute to the resonance properties of the metals. Consider a bilayer consisting of metals A and B. Let these electrons spend an average time τ_A in metal A before returning to metal B, and τ_B in metal B before returning to metal A. Under motional-narrowing conditions, the average g value $\bar{g}$ of the contributing electrons is the time-weighted average of the g values of the separate metals,

$$\bar{g}=\frac{\tau_A g_A+\tau_B g_B}{\tau_A+\tau_B}=\frac{N_A(\epsilon_F)g_A+N_B(\epsilon_F)g_B}{N_A(\epsilon_F)+N_B(\epsilon_F)}\ , \tag{2}$$

since $\tau_B/\tau_A=N_B(\epsilon_F)/N_A(\epsilon_F)$, as explained above.

The volume susceptibility of metal A, χ_A, is given by

$$\chi_A=g_A^2\mu_B^2 N_A(\epsilon_F)/V_A$$

and similarly for χ_B, where V is the volume of the metal. Thus for a bilayer consisting of metals A and B, having equal areas and respective thicknesses L_A and L_B,

$$\frac{N_B(\epsilon_F)}{N_A(\epsilon_F)}=\frac{\chi_B L_B/g_B^2}{\chi_A L_A/g_A^2}\ . \tag{3}$$

Substituting Eq. (3) into Eq. (2) yields Eq. (1).

Equation (1) is correct for infinite time averages and remains correct for averages over times long compared to τ_A and τ_B. The characteristic time in a CESR experiment is the transverse spin-polarization lifetime. Thus to observe a motionally narrowed CESR line, the characteristic transverse spin lifetime in a bilayer must be long compared to τ_A and τ_B.

Now consider a metal bilayer in which each Fermi-surface electron spends an equal time in each metal. In an applied magnetic field H_0, the electrons in metals A precess at a Larmor frequency ω_A, and those in metal B precess at ω_B, where $\omega=(g\mu_B/\hbar)H_0$. We can estimate when the difference in Larmor frequencies would cause an intrinsic broadening of the average precession frequency, $\bar{\omega}=(\bar{g}\mu_B/\hbar)H_0$. We define $\Delta\omega=(\omega_A-\omega_B)/2$. When an electron is in one material or the other for a time τ, its spin dephases by $\pm\Delta\omega\tau$ radians from $\bar{\omega}$. The usual result for a random walk applies: It takes n steps to move a distance $\lambda\sqrt{n}$, where λ is the step size. Thus the random hopping between the two metals results in a dephasing of one radian ($\sqrt{n}\,\Delta\omega\tau=1$) from $\bar{\omega}$ in a time $T_s=n\tau$. Solving for n yields $n=1/(\Delta\omega\tau)^2$. The observed linewidth is characterized by $1/T_s=\Delta\omega(\Delta\omega\tau)$. $1/T_s$ is less than $\Delta\omega$ by the factor $\Delta\omega\tau$. This is the motional-narrowing result: The observed line is narrower than the spread in frequencies (or, equivalently, g values) of the constituent spin systems. The requirement for obtaining a motionally narrowed line is that the transit time between metals be sufficiently short so that $\Delta\omega\tau<1$.

Now consider the influence of the CESR linewidths of each pure metal constituting the bilayer. Those linewidths are characterized by transverse spin-polarization lifetimes $(T_2)_A$ and $(T_2)_B$, respectively. If these lifetimes are long compared to the times τ_A and τ_B, an average transverse spin-polarized electron traverses the bilayer many times before it loses resonant spin energy to the lattice. Under these conditions the linewidth of the bilayer CESR is a weighted average of the linewidths of the constituents. It can be shown that the weighting factor is the same χ,L product as given in Eq. (3).

If, on the other hand, the spin lifetimes $(T_2)_A$ and $(T_2)_B$ are short compared to the τ's, the CESR averaging over the two spin systems will be incomplete. That is, the long-time average $\bar{g}$ in Eq. (1) is not attained in the CESR averaging time. Under these conditions the CESR line shape is broadened and distorted, and interpretation of a χ,L ratio is difficult. In practice, avoiding this condition imposes restrictions on the thicknesses of the metals.

To summarize, under *complete* motional-narrowing conditions ($\Delta\omega\tau\ll 1$), with spin lifetimes much longer than the average time a spin spends in each metal before crossing the interface, the position of a bilayer CESR line is given by Eq. (1). In this case $\bar{g}$ has a particularly simple dependence on the spin susceptibilities and thicknesses of the metals which constitute the bilayer.

B. Computer simulation

The previous simple model provides physical insight as to the dependence of $\bar{g}$ on the susceptibilities of the constituent metals. However, a computer simulation must be used for accurate data analysis, primarily because it can extract line-shape parameters under sample conditions for which motional narrowing is incomplete.

The computer simulation of CESR in a metal follows the phenomenological model proposed by Kaplan.[19] The diffusion-modified Bloch equations for the transverse components of magnetization,

$$\frac{d\vec{M}}{dt}=\gamma(\vec{M}\times\vec{H})-\frac{\vec{M}-\chi\vec{H}}{T_2}+D\nabla^2(\vec{M}-\chi\vec{H})\ ,$$

and two of Maxwell's equations,

$$\vec{\nabla}\times\vec{E}=-\frac{1}{c}\left[\frac{d\vec{H}}{dt}+4\pi\frac{d\vec{M}}{dt}\right]\ ,$$

$$\vec{\nabla}\times\vec{H}=\frac{4\pi\sigma}{c}\vec{E}\ ,$$

are solved simultaneously for each metal. $\vec{H}$ is the total instantaneous magnetic field (dc and rf), γ is the gyromagnetic ratio, D is the diffusion constant,[20] σ is the conductivity, and T_2 is the transverse spin-relaxation time.

The self-consistent solution of these equations results in two modes of propagation for transverse circularly polarized microwave fields in the metal: a normal skin-depth mode k_1, slightly modified by the magnetization carried by the electrons, and a spin-diffusion mode k_2. The k_2 mode is resonant at the CESR g value where it has a characteristic attenuation length $\delta_{\text{eff}}=(2DT_2)^{1/2}$, which is the mean distance a spin-polarized electron will diffuse in the transverse-spin relaxation time T_2. Under experimental conditions, k_1 corresponds to the anomalous skin-depth regime. However, this only introduces a phase shift in the TESR signal.[21]

To complete the simulation of CESR in bilayers, the k-vector solutions are solved exactly in both metals. These solutions are subject to the boundary conditions for the electromagnetic fields and the magnetization at the free surfaces and at the interface. At the free surfaces these boundary conditions are just the continuity of tangential $\vec{E}$ and tangential $\vec{H}$ and the requirement that the spin current $\vec{j}$ be 0 (assuming negligible surface relaxation). The spin current is related to the nonequilibrium magnetization, $\delta\vec{M}=\vec{M}-\chi\vec{H}$, by $\vec{j}=-(D/\gamma)\nabla\delta\vec{M}\cdot\hat{n}$. ($\hat{n}$ is the inward-pointing unit normal vector.) At the interface the continuity of tangential $\vec{E}$ and $\vec{H}$ still applies, but the boundary conditions for the spin current in each metal are more complicated. We employ the general linear relations between the nonequilibrium spin currents and spin densities first proposed by Flesner, Fredkin, and Schultz.[22] We have

$$-\frac{D_A}{\gamma_A}\vec{\nabla}(\delta\vec{M}_A\cdot\hat{n})=b_{11}\frac{\gamma_A}{\chi_A}\delta\vec{M}_A+b_{12}\frac{\gamma_B}{\chi_B}\delta\vec{M}_B\ ,$$
$$\frac{D_B}{\gamma_B}\vec{\nabla}(\delta\vec{M}_B\cdot\hat{n})=b_{21}\frac{\gamma_A}{\chi_A}\delta\vec{M}_A+b_{22}\frac{\gamma_B}{\chi_B}\delta\vec{M}_B\ . \tag{4}$$

In general the b coefficients may be complex. The Onsager relations give $b_{12}(\vec{H}_0)=b_{21}(-\vec{H}_0)$. In addition, our samples are polycrystalline, so there exists a plane of reflection symmetry parallel to $\vec{H}_0$. Under reflection, $\vec{H}_0$ changes direction, so $b_{21}(-\vec{H}_0)=b_{21}(\vec{H}_0)$, and thus $b_{12}=b_{21}$. Finally, positive entropy production requires $\text{Re}(b_{11})\text{Re}(b_{22})-\text{Re}^2(b_{12})\geq 0$, where $\text{Re}(x)$ means the real part of x. Flesner, Fredkin, and Schultz[22] have also shown experimentally that interfaces can be characterized with real b coefficients. Thus we take the interface boundary conditions to be given by Eq. (4) with real b_{ij}, $b_{12}=b_{21}$, and $b_{11}b_{22}-b_{12}^2\geq 0$.

The b's have simple physical interpretations in two limits. (1) In the limit of very weak coupling between the two metals, b_{12} describes the coupling, b_{11} characterizes the relaxation of spins striking the interface from metal A, and b_{22} characterizes the corresponding relaxation from metal B. In this case the system is characterized by three independent parameters. (2) In the limit of strong coupling between the two metals, b_{12} describes the coupling, but $b_{11}+b_{22}$ is a single parameter characterizing the relaxation of spins. This is the motional-narrowing case. It does not matter from which direction a spin strikes the interface when the spin lifetime is sufficiently long to achieve motional narrowing. In this case the system is characterized by two independent parameters. For the strongly coupled case, Fredkin[18] has suggested a simple kinetic model to express the b coefficients in terms of two more physically meaningful parameters, P and Q.[23] Q is the probability that an electron's spin relaxes when striking the interface, and P is the probability that it crosses the interface.

Combining the boundary conditions with the Kaplan solutions yields 10 coupled equations. The transmitted microwave field, corresponding to the TESR signal,[24] is then determined by solving the 10×10 matrix equations.

III. EXPERIMENT

A. Technique

TESR experiments were performed with the use of an X-band superheterodyne spectrometer. A block diagram of this spectrometer is shown in Fig. 2. In the spectrometer microwave power is amplitude modulated at an audio frequency and coupled into one of a pair of cavities, the transmit cavity (TC). A sample forms the common wall between the two cavities, which are filled with the dielectric material Lucalox (polycrystalline Al_2O_3), and operate in the TE_{101} mode near 9.2 GHz. If the cavities are sealed sufficiently well, any power detected in the receive cavity (RC) is power that has been transmitted through the sam-

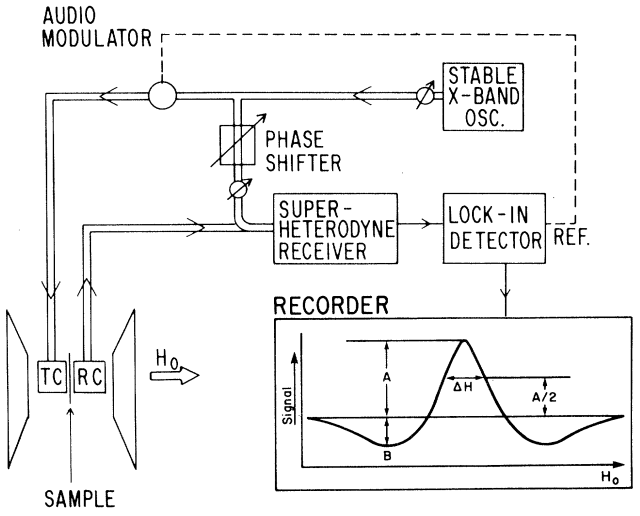

FIG. 2. Block diagram of the TESR technique. TC and RC are the transmit cavity and receive cavity, respectively. TESR line-shape parameters, for a symmetrical line are also depicted in the figure, with ΔH being defined as the full linewidth at half the positive-going amplitude ($A/2$). All bilayer samples studied satisfied $A \gg B$ below 15 K.

ple. This power is coupled out of the RC and into a superheterodyne receiver. In the receiver, strong microwave reference power (unmodulated) is added to the weak transmitted power (modulated) to (i) bias the intermediate frequency (if) detector at an optimum level and (ii) provide a reference microwave field that is much larger than the microwave field coupled out of the receive cavity. This allows one to observe either the in-phase or out-of-phase components of the transmitted field by an appropriate choice of the phase of the reference field. The audio-frequency output of the if detector is fed into a lock-in detector whose output is recorded as a function of applied dc magnetic field. We refer to this output as the signal.

According to our model, $\bar{g}$ is independent of the orientation of the dc magnetic field. Further, at sufficiently low temperatures, where conductivity and linewidth are temperature independent, $\bar{g}$ should be independent of temperature. Data were taken for all samples at several low temperatures, typically 5, 10, and 15 K, and at various magnetic field angles to ensure other properties of the metals had not influenced the observed signal characteristics. For each temperature and magnet angle, the phase of the reference field was adjusted so the TESR signal was symmetrical (tuning to χ''). This allowed accurate measurements of the g value, linewidth (ΔH), and A/B ratio of the bilayer TESR signal (see Fig. 2 for an illustration). NMR field markers were used to calibrate the magnetic field sweep. The magnetic field at the sample was determined by reflection CESR on a neutron-irradiated lithium-fluoride g marker located inside the RC. With this procedure we determined the g value for most samples to within three parts in 20 000, or ± 0.5 G.

B. Sample preparation and properties

Two types of bilayer samples were prepared: (i) evaporated alkali films on Cu or Ag foils, and (ii) electroplated Cu on Ag foils.

All of the Cu and Ag foils used for the bilayers were 99.9999%-pure material supplied by Cominco, rolled to nominal thicknesses of 0.7 and 1.0 mil, and subsequently oxygen-annealed. Oxygen annealing decreases the low-temperature resistivity and narrows the CESR linewidth. The resistivity ratio of the Cu and Ag foils, $\rho 300\ \mathrm{K}/\rho 4.2\ \mathrm{K}$, was ~ 1500 and the residual linewidth (ΔH below 10 K) was ~ 10 G. The average thickness of each foil was determined to an accuracy of $\sim 2\%$ from its known mass density[25] (see Table I), and its measured weight and area. The g values of the metals used in our bilayers are also presented in Table I. We determined the g value of our silver foils to be $g = 1.9831 \pm 0.0002$. The g values of the other metals (except Li) are known from previous measurements in our laboratory.[26,27] We used VanderVen's g value for lithium.[28]

The alkali-metal films were deposited on the Cu or Ag foils by electron-beam evaporation at a pressure of about 2×10^{-6} Torr. Typical evaporation rates were 500—1000 Å/sec. Thicknesses were determined to an accuracy of roughly 5% by a quartz-crystal oscillator placed in a position symmetric with the bilayer sample above a crucible containing the alkali metal. After deposition of the alkali-metal film, a ~ 5-μm-thick coating of wax was evaporated to protect the alkali metal during its subsequent brief exposure to the atmosphere. In addition to evaporation onto the Cu or Ag foil, alkali metal was simultane-

TABLE I. Important parameters characterizing the bulk properties of the metals used in our bilayer studies.

	Li	Na	K	Cu	Ag
Bulk contraction to 5 K (%)	−0.8[a]	−1.43[b]	−1.72[c]	−0.326[b]	−0.413[b]
Contraction of film constrained in two dimensions (%)	−2.32±0.20	−4.15±0.36	−4.99±0.43	−0.95±0.1	−1.20±0.1
Contraction used to calculate final thicknesses (%)	−1.56±0.76	−2.79±1.36	−3.36±1.64	−0.64±0.31	−0.80±0.40
Room-temperature mass density[d] (g/cm^3)	0.534	0.971	0.862	8.93	10.50
Free electron χ at 5 K (10^{-6} cgs volume units)	0.801	0.660	0.533	0.975	0.863
g value	2.002 26[e] ±0.000 002	2.001 40[f] ±0.000 05	2.000 05[f] ±0.000 05	2.0325[g] ±0.0005	1.9831 ±0.0002
Effective mass, m^*/m	2.21[h] ±0.07	1.24[i] ±0.02	1.21[i] ±0.02	1.383[j] ±0.002	1.004[j] ±0.002

[a]Reference 31.
[b]Reference 30.
[c]Reference 32
[d]Reference 25.
[e]Reference 26.
[f]Reference 27.
[g]Reference 28.
[h]Reference 43.
[i]Reference 42.
[j]Reference 41.

ously deposited on an adjacent mica substrate. This allowed subsequent measurement of the CESR g value and linewidth, and the resistivity ratio of the evaporated alkali-metal film. All evaporated alkali-metal films had resistivity ratios of ~ 400 (Li) or ~ 1000 (Na and K), and low-temperature (< 10-K) linewidths ΔH of $\simeq 1$ G. Samples were electrically sealed between the cavities with a 3-mil annealed copper wire O-ring. This prevented microwave leakage between the cavities and avoided squeezing of the alkali-metal film exposed to the microwaves.

We found that the best interface between the alkali-metal film and copper or silver foil, from the standpoint of a motionally narrowed CESR line, was obtained by argon-ion-milling the foil surface for about 5 min at an ion-beam current of 0.1 mA/cm^2 and a voltage of 6 kV. This process removed roughly 1000 Å of material. Evaporation of the alkali metal was begun with a shutter shielding the sample while the ion milling continued. The shutter was removed immediately *before* the ion beam was turned off. We found this sequence to be important for producing bilayer samples with strong spin coupling between the two metals. The spin-relaxation probability Q at the bilayer interface was typically $\sim 1.5 \times 10^{-3}$.

Bilayers consisting of copper on silver were made by electroplating Cu onto one side of a clean silver foil using a high-purity copper sulfate bath. Visual inspection suggests that the deposition of copper on the silver foil occurred epitaxially, producing an interface and copper film with most desirable properties. The spin-relaxation probability Q at the Cu-Ag interface was very small ($< 2 \times 10^{-4}$), and a narrow CESR linewidth was obtained. Preferentially etching[29] the silver from the copper enabled us to measure the resistivity ratio and linewidth of the electroplated Cu. A resistivity ratio of ~ 300 and a linewidth ΔH of $\simeq 20$ G was typical. The sample and anode geometry we used provided a uniform-plated Cu film. For the plated Cu films we determined the average copper thickness to an accuracy of $\sim 5\%$ (by the ratio of mass to area).

C. Determination of sample thickness

In Sec. III B we indicated the methods used for the determination of sample thicknesses and the uncertainty involved with each method. Since an accurate measure of thickness is essential for obtaining accurate susceptibilities, we now discuss the thickness determinations in greater detail.

As mentioned previously, the thicknesses of the copper and silver foils and of the electroplated copper films were determined from precise mass and area measurements. This measured the average thickness of each sample. Using a precision micrometer, which gives reading to an accuracy of $\simeq 0.5$ μm, we determined that thickness variations over the sample dimensions (1.4 cm $\times$ 1.2 cm) were no more than 10%. Since conduction electrons sample the average thickness of each metal in the bilayer, the average thickness is the quantity we needed for our experiments.

Thicknesses of the evaporated alkali metals were measured with a quartz-crystal oscillator arranged as described in Sec. III B. For evaporations onto copper foils, gold-coated crystals subsequently plated with copper were used; for evaporations onto silver foils, silver-coated crystals were used. This was done to ensure the same sticking coefficient for the alkali to both the crystal and the sample.

Calibration checks were made to determine the accuracy of the crystal oscillator and the uniformity of the evaporation pattern from the hearth. For calibration, silver, copper, and lithium were each evaporated onto clean, dry glass cover slips and the oscillator simultaneously. The mass of the film on a cover slip was determined (a) by dissolving the metal into solution and measuring its concentration with atomic absorption spectroscopy (lithium), (b) by measuring the mass of the cover slip before and after the evaporation of the metal (copper), or (c) by both methods (silver). With the use of the known area of coverage on the cover slips and the bulk mass densities listed in Table I, room-temperature thicknesses were then determined. These calibrations indicated that the thicknesses were uniform to within $\pm 5\%$ over an area approximately twice that used to make the bilayers and monitor the thicknesses. The crystal oscillator agreed with the calibration measurements to within $\pm 5\%$.

We corrected our measured room-temperature sample thicknesses for thermal contraction to the low temperature of the experiment. Bulk thermal contractions were obtained from the literature (Table I).[30–32] However, we know from measurements on sodium, potassium, and rubidium in this laboratory[33] that metal films constrained to contract in one dimension contract much more than bulk metals. From these measurements we inferred a general relation from room temperature to 77 K between the contraction of bulk materials and the contraction of materials constrained to shrink in one dimension. The ratio of the constrained contraction to the bulk contraction is 2.9 ± 0.25. This ratio was assumed to be valid down to 5 K and to be correct for all the metals we used. We do not know how constrained each constituent of the bilayer was since each bilayer was mounted between a pair of massive brass cavities which also contracted as the temperature was lowered. So we used the average between bulk contraction and that for a film constrained to contract in one dimension, with an assigned error spanning these limits. These data are summarized in Table I. We note that only an error in the thickness ratio of the two constituents of a bilayer affects the measured susceptibility ratio. Thus, if we had neglected thermal contractions, the largest error we would have introduced into the susceptibility ratio would be $\sim 2.7\%$ (for the potassium-copper bilayers, since potassium and copper have the largest differential contraction among the metals used in these experiments).

IV. RESULTS

A. Computer simulations

The computer simulation of the bilayer TESR signal was discussed in Sec. II. To summarize, the computer solves Kaplan's[19] equations in both metals, subject to the boundary conditions at the free surfaces and the interface. For a unit-amplitude incident-microwave field, the com-

puter calculates the transmitted-field amplitude as a function of the dc field $\vec{H}_0$. The computer-simulated bilayer TESR signal is characterized by a g value, linewidth, and A/B ratio (Fig. 2) whose values depend on three independent parameters. These are the interface parameters P and Q from Fredkin's kinetic model, and the spin susceptibility ratio of the metals constituting the bilayer, χ_B/χ_A. Q primarily affects the linewidth, while P affects the A/B ratio, and, under conditions of incomplete motional narrowing, the g value. χ_B/χ_A directly affects the g value as evidenced by Eq. (1). These three parameters were varied to fit the computer-generated line to the experimental TESR data. A unique value of χ_B/χ_A was thus obtained with an uncertainty dependent upon the experimental errors associated with the A/B ratio and quantities contained in Eq. (1). The advantage of the computer simulation is that it correctly models sample conditions with incomplete motional narrowing, in which case an analysis with Eq. (1) would be inappropriate.

B. Systematic checks

Sample conditions were varied to check for systematic errors. For some samples, the thicknesses of the alkali and copper were varied holding their ratio fixed. This is a check of motional narrowing and more generally a check of unanticipated geometric effects. The ratio of the χ,L product was also varied. This changes the bilayer $\bar{g}$ value. These tests confirmed invariance of the measured χ ratio under different averaging conditions. In addition, data were taken at three temperatures and three magnet angles. The former allowed a determination of the upper limit of the susceptibility contribution of any local-moment impurity in the sample, while the latter checked for unanticipated effects of spin relaxation at the sample boundaries.[34] These spin-relaxation effects can occur when the spin-diffusion length δ_{eff} is comparable to the size of the cavity or when $B_0\omega\tau\sim 1$. Under these conditions, the g values and linewidths observed with CESR can vary as the direction of $\vec{H}_0$ is changed with respect to the sample normal. These effects are minimized when $\vec{H}_0$ is perpendicular to the sample surface. The bilayer TESR data taken versus magnet angle showed no shift in $\bar{g}$ even though there was a small angular dependence to the linewidth.

Copper readily accepts local-moment impurities which could significantly affect the observed $\bar{g}$ at very low impurity concentrations. One consequence is that the effective χ of the Cu would be the sum of χ_{Cu} and χ of the local moment. A second consequence is that the g value of the observed resonance in copper would shift in a manner very similar to the frequency-averaging in Eq. (1) weighted by the χ's and g's of copper and the local-moment impurity.[15] The local-moment susceptibility has a $1/T$ temperature dependence, and thus the effective Cu g value would be temperature dependent. From the known resistivity increments of local moments in Cu and Ag and the measured resistivity ratio of the bulk copper, we determined the maximum concentration of local-moment impurities in our Cu and Ag foils. We used these maximum impurity concentrations to estimate the maximum shifts in the values of the χ's for Cu and Ag that could be consistent with our bilayer measurements. As an example of this analysis, resistivity-ratio measurements on annealed 10-mil copper foils of the same material used for the bilayers are consistent with a maximum of 0.77 ppm of manganese impurities. For 1 ppm of manganese in copper at 5 K, the effective electron-spin susceptibility is approximately 6% greater than the χ of pure copper. At 15 K, however, the susceptibility is enhanced by only about 2% and the effective g value for Cu reduced by 0.5%. Taking into account both of these effects, we determined that 1 ppm of Mn in Cu would have resulted in a 2% change in the value of χ of Cu deduced from bilayer measurements.

C. Error analysis

Errors in calculating χ result from uncertainties in the input parameters used to model the bilayer on the computer. The use of Eq. (1) for the resonant $\bar{g}$ value allows a simple first-order analysis of errors. All errors quoted in this paper are standard deviations from the mean.

We define

$$Z=\frac{g_A^2L_B\chi_B}{g_B^2L_A\chi_A}=\frac{g_A^2L_B}{g_B^2L_A}\chi_R\ .$$

Equation (1) then becomes

$$\bar{g}=\frac{g_A+Zg_B}{1+Z}\ .$$

Let $\Delta g=g_B-g_A$. It can be shown that

$$\left[\frac{\sigma(\chi_R)}{\chi_R}\right]^2\simeq\left[\frac{(1+Z)^2}{Z}\frac{\sigma(\bar{g})}{\Delta g}\right]^2+\left[\frac{\sigma(L_A)}{L_A}\right]^2+\left[\frac{\sigma(L_B)}{L_B}\right]^2+\left[(1+Z)\frac{\sigma(g_B)}{\Delta g}\right]^2+\left[\frac{(1+Z)}{Z}\frac{\sigma(g_A)}{\Delta g}\right]^2,$$

where $\sigma(Y)$ is the standard-deviation error in Y. The validity of these expressions was verified with the computer simulation for the maximum errors in the sample-dependent and material-dependent parameters. In addition, the simulation was used to verify that χ_R was insensitive to uncertainties in resistivity ratios and linewidths of the constituent metals.

The effects of all experimental uncertainties mentioned have been included in the χ_R's listed in Table II. The list-

TABLE II. Final bilayer susceptibility ratio results.

Bilayer			Number of bilayers
Metal A	Metal B	$\chi_R=\chi_B/\chi_A$	measured
Li	Cu	0.590±0.021	7
Na	Cu	1.30 ±0.06	3
K	Cu	1.45 ±0.09	3
Na	Ag	0.857±0.039	3
K	Ag	0.942±0.059	2
Cu	Ag	0.616±0.036	2

ed χ_R for a given type of bilayer is a weighted average of two or more measurements, where the result of each measurement was weighted inversely by its own variance σ_i^2. The final error was calculated on both an externally consistent (given by the standard deviation spread of the measurements), and an internally consistent $[(\sum\sigma_i^{-2})^{-1}]$ basis.[35] For each χ_R the listed error is the larger of the two.

D. Least-squares determination of absolute spin susceptibilities

Since they are measurements of susceptibility ratios, the results listed in Table II are not sufficient to determine the absolute spin susceptibilities of the metals studied. To determine absolute spin susceptibilities, at least one absolute measurement must be taken from other experimental data (e.g., spin-wave or dHvA data). A least-squares procedure can then be used to determine the absolute susceptibilities which best fit the combined experimental data.

Each experimental χ ratio listed in Table II can be regarded as an experimental equation relating five independent variables (the absolute susceptibilities of Li, Na, K, Cu, and Ag). Absolute measurements(s) obtained from other experiments become additional equations. This results in a minimum of seven equations for five unknowns, a measurement error being associated with each equation. Thus we have an overdetermined system of equations. We obtained a least-squares solution to these equations following the methods of Taylor *et al.*[35] Briefly, the equations were linearized around initial values of the dependent variables. The initial values were chosen to be nearly equal to the expected final values. A least-squares solution was then obtained by minimizing the sum of squares of the normalized residuals, which are defined in the usual way, but weighted inversely by the associated measurement error.

Table III lists the susceptibilities resulting from the least-squares analysis of the six measurements listed in Table II with the use of various combinations of absolute susceptibility measurements of Na and/or K obtained from either spin-wave or dHvA measurements. The results listed in column (a) of Table III used the spin-wave results of Dunifer *et al.*[5] as input. For this case the susceptibilities of Na and K were treated as dependent variables. The major reasons for taking the Na and K values to be adjustable are (1) there is significant experimental uncertainty associated with the spin-wave values, and (2) it allowed us to check the consistency of our data with the spin-wave data (by analyzing the final residuals). The results listed in column (b) are from the use of the best dHvA susceptibility values of Na (Ref. 10) and K (Ref. 9) which, due to their relatively small measurement errors,[36] were held fixed in the analysis. (Allowing the values to vary would have produced essentially the same results.) The results listed in column (c) used only the susceptibility of K, since spin-wave and dHvA measurements agree so well for K, but differ somewhat for Na. Here again the susceptibilities of Na and K were treated as dependent variables. Since the dHvA and spin-wave measurements of K so closely agree, we conclude from the resulting value for Na that the spin-wave susceptibility measurement of Na is more compatible with our data than is the dHvA value.

The susceptibilities and associated errors listed in the last column of Table III are our final results. They are a simple average of the results in columns (a)—(c). In all cases, our analysis of the resulting residuals indicates that each measurement listed in Table II is compatible with the other five measurements and with the spin-wave and dHvA measurements, indicating the reliability of our method.

It is important to realize that since our method measures spin-susceptibility ratios, a systematic error in the thickness or g-value measurement of a given metal whose χ we wish to determine would not become apparent in our least-squares analysis. However, such an error would affect only the resulting χ of the given metal; it would have no effect on the susceptibility determinations of the other metals. But, if such an error occurred for a metal used as an absolute standard (i.e., Na or K), it would affect the susceptibility determination of all the remaining metals, *including* other standards. Thus, if more than one standard were used in the least-squares analysis (as we have done), such a systematic error *would* become apparent. Our results indicate that no systematic error occurred for the Na or K metals we used as standards.

TABLE III. Final results for χ (10^{-6} cgs units) obtained by combining our bilayer data listed in Table II with various susceptibility measurements of Na and K, referred to as additional input data.

	(a) Spin wave	(b) dHvA	(c)	(d) Final results
Additional input data				
Na	1.042±0.044	1.076±0.005		
K	0.900±0.031	0.904±0.003	0.902±0.016	
Final output data				
Cu	1.350±0.059	1.388±0.047	1.322±0.070	1.35±0.06
Ag	0.861±0.037	0.885±0.029	0.843±0.044	0.86±0.04
Li	2.289±0.130	2.354±0.118	2.240±0.143	2.29±0.13
Na	1.028±0.036		0.999±0.059	
K	0.908±0.028			

V. DISCUSSION

A. Comparison with theory and other experiments

The results of these experiments for the susceptibilities of copper, silver, and lithium are compared with other measurements and theoretical predictions in Table IV. The data have been reexpressed in terms of susceptibility enhancements χ/χ_0. The free-electron susceptibilities at 5 K are listed in Table I.

Prior to our work, the only experimental measurements of the susceptibility enhancements in copper and silver were the dHvA measurements of Bibby and Shoenberg[11] and Randles.[37] They measured the absolute amplitude of the dHvA oscillations for several orbits on the Fermi surface. Bibby and Shoenberg took simple arithmatic averages over the $\langle 100 \rangle$ and $\langle 111 \rangle$ orientations in obtaining their results for copper and silver, while Randles took an average over the whole Fermi surface in obtaining his result for copper.

For lithium, direct measurements of the susceptibility have been obtained by "area under the curve" CESR measurements and by the determination of transport coefficients in the completely damped spin-wave regime ($|B_0\omega\tau| \ll 1$). The area under the curve measurement is an extremely difficult one requiring integration of a Lorentzian line over $6\frac{1}{2}$ linewidths to include 90% of the area. Only the most recent measurement, by Whiting, VanderVen, and Shumacher,[2] is listed in Table IV. This procedure is unlikely to be applicable to metals other than lithium and sodium. Flesner and Schultz[7] and Witt and VanderVen[8] have determined the many-body-enhanced diffusion constant for lithium and sodium from line-shape analysis in the case of completely damped spin waves. However, uncertainties of this method are considerable. Witt and VanderVen mention that their measurement for sodium is suspect. For lithium, the Witt and VanderVen result is listed in Table IV along with a measurement by Flesner and Schultz[7] obtained in the partially damped spin-wave regime. The latter measurement required effective-mass data to determine a susceptibility enhancement.

All theoretical predictions[38–40] were adjusted to include the factor $(g_s/g_0)^2$ which enters into the susceptibility enhancement. The theoretical values of χ/χ_0 were obtained from the relation

$$\chi/\chi_0=(g_s/g_0)^2[n(\epsilon_F)/n_0(\epsilon_F)][1-n(\epsilon_F)I]^{-1},$$

where $n(\epsilon_F)$ is the density of states at the Fermi energy in the metal, $n_0(\epsilon_F)$ is the free-electron density of states, and I is an exchange-correlation parameter. Values of $n(\epsilon_F)$ and I were taken directly from the authors's tabulated values,[38,40] while $n_0(\epsilon_F)$ was calculated from their quoted lattice constants. For lithium, the value of χ/χ_0 was taken directly as quoted.[39]

Within the errors of the measurements there is very satisfactory agreement between our TESR bilayer results for Ag and Li, those obtained by the other methods listed in Table IV, and the most recent theoretical predictions of MacDonald *et al.*[38,39] For Cu, although our value is somewhat lower than the dHvA results and the referenced theoretical values[38,40] we believe the discrepancies are within the uncertainties.

Using the relation

$$\chi/\chi_0=(g_s/g_0)^2(m^*/m)(1+B_0)^{-1}$$

and the effective masses[41–43] listed in Table I, we have determined the many-body parameter B_0 for Cu, Ag, and Li from our measured susceptibility enhancements. For copper we obtain $B_0=0.025\pm0.04$ and for silver $B_0=-0.015\pm0.04$. These results compare favorably with the results obtained by Lubzens *et al.*[44] of $|B_0| \leq 0.06$ for Cu and Ag. For Li we obtain $B_0=-0.23\pm0.05$, which agrees with the partially damped spin-wave result by Fles-

TABLE IV. χ/χ^0 results: Comparison with other experiments and theory.

	Cu	Ag	Li
Our bilayer results	1.39±0.06	1.00±0.04	2.86±0.16
dHvA Bibby *et al.*[a]	1.50±0.02	1.05±0.07	
Randles[b]	1.49		
CESR area[c]			2.74±0.05
Spin waves			
completely damped[d]			2.86±0.7
partially damped[e]			2.84±0.1
Theory			
McDonald *et al.*[f]	1.55	1.02	2.91
Janak[g]	1.55	1.12	3.36

[a]Reference 11.
[b]Reference 37.
[c]Reference 2.
[d]Reference 8.
[e]Reference 7.
[f]References 38 and 39.
[g]Reference 40.

ner *et al.*[7] of $B_0=-0.23\pm0.03$ (analyzed taking $m^*/m=2.21$).

B. Future applications

In this work we have used the measured susceptibilities of Na and K as standards to self-consistently determine the susceptibilities of Cu, Ag, and Li. Consistency of our results suggests that this is a reliable measurement technique, which may be expanded to include other metals for which CESR can be observed. In addition, copper and silver can now be used as susceptibility standards for future bilayer measurements. They are superior elements for bilayer susceptibility measurements since their g values differ significantly from those of most other metals of interest, allowing more sensitive measurements of the χ's of these metals. Also, Cu and Ag are much less reactive than the alkali metals, and thus compatible with more materials as a constituent in a bilayer.

Elements which are interesting candidates for future bilayer CESR susceptibility determinations include aluminum and niobium,[45] both of which are superconductors, palladium, whose susceptibility enhancement is believed to be quite large[46] $[(m^*/m)/(1+B_0)\sim25]$, and magnesium, for which theoretical calculations of the susceptibility have been made.[47] Measurement of the susceptibility of beryllium would also be of interest, since recent theoretical predictions[47] disagree with available experimental data[48–50] by roughly a factor of 2.5. But, to our knowledge, no beryllium foil has been prepared with a sufficiently high purity to enable the observation of a transmission CESR signal. We also note that making measurements on these elements for as many different bilayer combinations as possible (e.g., CuAl, AgAl, etc.), would not only determine the susceptibilities of these elements but would also reduce the errors in the susceptibilities of Cu, Ag, and Li by the use of the self-consistent least-squares analysis for all bilayer experimental data.

Finally, we mention the possibility of observing CESR in a bilayer consisting of one element in which a CESR signal has been observed, and one in which it has not. We have tried this for 15-μm-thick 99.9999%-purity gold foils, which exhibit no observable CESR signal by themselves, but when plated with roughly 15-μm of copper produce a broad ($\Delta H\sim200$ G) bilayer TESR signal. In principle, one could determine both the g value and susceptibility of a metal of interest by varying the relative thicknesses of the two metals constituting the bilayer, although the errors might be substantial.

ACKNOWLEDGMENTS

We wish to thank Professor D. R. Fredkin for many helpful conversations, and Professor S. H. Vosko for copies of unpublished manuscripts and stimulating conversations. This work was supported by the National Science Foundation under Grant No. NSF-DMR-80-07969. We also wish to thank the University of California, San Diego (UCSD) Academic Senate Committee on Research for its support.

---

*Present address: Bell Laboratories, Holmdel, NJ 07733.

[1]$\chi_0=(g_0\mu_B^2/4)n(\epsilon_F)$, where g_0 is the free-electron-spin g value equal to 2.0023, μ_B is the Bohr magneton, and $n(\epsilon_F)$ is the free-electron density of states at the Fermi surface.

[2]B. R. Whiting, N. S. VanderVen, and R. T. Schumacher, Phys. Rev. B 18, 5413 (1978).

[3]See Ref. 5 for a discussion of these theories.

[4]I. M. Lifshitz and A. M. Kosevitch, Zh. Eksp. Teor. Fiz. 29, 730 (1955) [Sov. Phys.—JETP 2, 636 (1955)].

[5]G. L. Dunifer, D. Pinkel, and S. Schultz, Phys. Rev. B 10, 3159 (1974).

[6]D. Pinkel and S. Schultz, Phys. Rev. B 18, 6639 (1978).

[7]L. D. Flesner and S. Schultz, Phys. Rev. B 14, 4759 (1976).

[8]C. E. Witt and N. S. VanderVen, Phys. Rev. B 19, 887 (1979).

[9]B. Knecht, J. Low Temp. Phys. 21, 619 (1975).

[10]J. M. Perz and D. Shoenberg, J. Low Temp. Phys. 25, 275 (1976).

[11]W. M. Bibby and D. Shoenberg, J. Low Temp. Phys. 34, 659 (1979).

[12]D. L. Randles, Proc. R. Soc. London Ser. A 331, 85 (1972).

[13]Li exhibits no dHvA effect at low temperatures presumably because it undergoes a martensitic transformation to a mixture of crystalline phases at liquid-nitrogen temperatures. However, the dHvA effect has been observed in lithium-metal dispersions in which the martensitic transformation is suppressed. See D. L. Randles and M. Springfield, J. Phys. F 6, 1827 (1976).

[14]P. Monod and S. Schultz, Phys. Rev. 173, 645 (1968).

[15]S. Schultz, M. R. Shanabarger, and P. M. Platzman, Phys. Rev. Lett. 19, 749 (1967).

[16]M. R. Shanabarger, Ph.D. Thesis, University of California, San Diego, 1970 (unpublished).

[17]For a discussion of the TESR technique and its benefits see S. Schultz, in *Measurements of Physical Properties,* edited by E. Passaglia (Wiley, New York, 1972), Vol. IV, Chap. V B.

[18]D. R. Fredkin (private communication).

[19]J. I. Kaplan, Phys. Rev. 115, 575 (1959).

[20]The addition of many-body interactions in metals modifies the diffusion constant D. This is included in our calculations, but has no significant effect on our results and will not be discussed.

[21]M. Lampe and P. M. Platzman, Phys. Rev. 150, 350 (1966).

[22]L. D. Flesner, D. R. Fredkin, and S. Schultz, Solid State Commun. 18, 207 (1976).

[23]This model is presented in L. D. Flesner, Ph.D. thesis, University of California, San Diego, 1976 (unpublished), Appendix I.

[24]This procedure is described in detail in Appendix II of Ref. 23.

[25]Bulk mass densities taken from *Handbook of Chemistry and Physics* (Chemical Rubber Co, Cleveland, Ohio, 1970).

[26]G. L. Dunifer, Ph.D. thesis, University of California, San

Diego, 1968 (unpublished).

[27]D. Lubzens, Ph.D. thesis, University of California, San Diego, 1975 (unpublished). The g value is consistent with $g_{Cu}=2.0328\pm0.001$, obtained by A. Stesmans, J. von Meijel, and S. P. Braim, Phys. Rev. B 19, 5470 (1979).

[28]N. S. VanderVen, Phys. Rev. 168, 787 (1968).

[29]The etching solution consisted of $\frac{1}{4}NH_4OH+\frac{1}{4}H_2O_2+\frac{1}{2}H_2O$ at room temperature.

[30]R. J. Corruccini and J. J. Gniewick, in *Thermal Expansion of Technical Solids at Low Temperatures,* Natl. Bur. Stand. (U.S.) Spec. Publ. No. 29 (U.S. G.P.O., Washington, D.C., 1961).

[31]*Thermal Expansion: Metallic Elements and Alloys,* Vol. 13 of *Thermophysical Properties of Matter,* edited by Y. S. Touloukian (Plenum, New York, 1975).

[32]See Ref. 5. The bulk contraction was obtained from the 5-K lattice constant and the room-temperature mass density in Ref. 25.

[33]D. Pinkel, Ph.D. thesis, University of California, San Diego, 1974 (unpublished).

[34]J. F. Dobson, Phys. Lett. A 44, 171 (1973).

[35]For a more complete discussion of error analysis and least squares, see B. N. Taylor, W. H. Parker, and D. N. Landenberg, Rev. Mod. Phys. 41, 375 (1969), in particular Secs. II A 4, III A, and III B 1.

[36]The small measurement errors quoted for the dHvA results reflect only experimental uncertainties and do not account for uncertainties associated with the application of Fermi-liquid theory in the interpretation of dHvA data.

[37]See Ref. 12. The result quoted by Randles was $\chi/\chi^0=1.45$. We believe he neglected the factor $(g_s/g_0)^2$ in obtaining his result. The value listed in Table IV includes this correction.

[38]A. H. MacDonald, J. M. Daams, S. H. Vosko, and D. D. Koelling, Phys. Rev. B 25, 713 (1982).

[39]A. H. MacDonald, K. L. Lui, S. H. Vosko, and L. Wilk, Can. J. Phys. 59, 500 (1981).

[40]J. F. Janak, Phys. Rev. B 16, 255 (1977).

[41]D. L. Martin, Phys. Rev. B 8, 5357 (1973). These specific-heat effective masses are consistent with the cyclotron masses obtained by B. Lengeler, W. R. Wampler, R. R. Bourassa, K. Mika, K. Wingerath, and W. Velhoff, Phys. Rev. B 15, 5493 (1977).

[42]C. C. Grimes and A. F. Kip, Phys. Rev. 132, 1991 (1963).

[43]Obtained from the specific-heat data summary of N. E. Phillips [Solid State Sci. 2, 467 (1971)]. The assigned error roughly indicates the spread of Phillips's listed values of γ.

[44]D. Lubzens, M. R. Shanabarger, and S. Schultz, Phys. Rev. Lett. 29, 1387 (1972).

[45]CESR has recently been observed in niobium D. Vier and S. Schultz, Phys. Lett. (in press).

[46]P. Monod, J. Phys. (Paris) Colloq. 39, C6-1472 (1978).

[47]L. Wilk, W. R. Fehlner, and S. H. Vosko, Can. J. Phys. 56, (1978).

[48]G. Feher and A. F. Kip, Phys. Rev. 98, 337 (1955).

[49]J. H. Orchard-Webb, A. J. Watts, M. A. Smithard, and J. E. Cousins, Phys. Status Solidi 41, 325 (1970).

[50]C. S. Bowring and V. T. Wynn, Phys. Lett. 33A, 401 (1970).